Chapter V: Application of Fiber Bragg Grating

5.1 Introduction

Fiber Bragg gratings (FBGs) have emerged as important components in a variety of lightwave applications. They are used in many devices such as erbium-doped fiber amplifiers (EDFA) [1], fiber lasers [2], Raman amplifiers [3], wavelength division multiplexers (WDM's) demultiplexers [4], add/drop multiplexers [5] and dispersion compensators [6] because they have a unique filtering property and versatility as an in-fiber device. In this chapter, the utilisation of the FBG in a gain-clamped EDFA and a fiber laser, is studied.

EDFA is one of the critical devices in a WDM system. WDM and EDFA are key technologies to the new generation of high speed and large capacity telecommunication systems. However, the optical gain of a conventional EDFA depends on many parameters such as the input signal level, the pump power and signal wavelength. This can cause signal power instability and cross talk between different channels in multi wavelength optical networks where the total number of channels or the total signal power in the network varies when channels are added or dropped [7]. The ability to automatically control EDFA gain is essential for the design of optical networks using in line EDFAs. One effective method for achieving this is to introduce a laser at a particular wavelength in the EDFA so that a constant average population inversion can be maintained because of the homogenous broadening nature of the EDFA gain medium. In the next section, a FBG is used to provide an optical feedback in the cavity. The effect of the pump power,

input signal power and optical feedback power attenuation on the amplifier performance parameters such as output signal power, signal gain and noise figure are studied in the section.

Erbium-doped silica fiber can be used to make fiber lasers capable of operating in the wavelength of around 1.55μm. The two main ingredients of a laser are a gain medium that provides amplification and a suitable cavity that provides optical feedback [8][9][10]. Optical gain is realized when the laser medium is pumped optically to achieve population inversion. In this report, a three level laser system is used since an erbium-doped fiber is utilized as a gain medium. In section 5.3, a fiber laser with a different reflectivity FBG as an optical feedback is studied and compared. The laser characteristics such as threshold pump power, slope efficiency etc are investigated. Laser tuning also is demonstrated in the section.

5.2 Gain-clamped erbium-doped fiber amplifier

5.2.1 Experimental set up

The experimental set-up of the FBG-clamped EDFA system is shown in Figure 5.1. The system consists of an isolator, coupler, 980/1550nm wavelength division multiplexer (WDM), erbium-doped fiber (EDF), circulator, FBG and an attenuator. The system uses a ring laser configuration. The output of the EDFA is split into an output branch and a feedback branch by a circulator with the FBG placed at the output end of the amplifier. The laser wavelength λ_L is chosen at 1552.6, which corresponds to the center wavelength of FBG. Reflection profile of the FBG is shown in Figure 5.2. It has a peak wavelength at 1552.6nm and a reflectivity of approximately 70%. The reflected part of

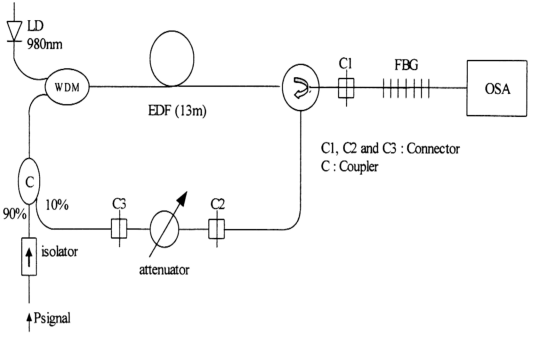

Figure 5.1: Experimental set-up of FBG-clamped amplifier system

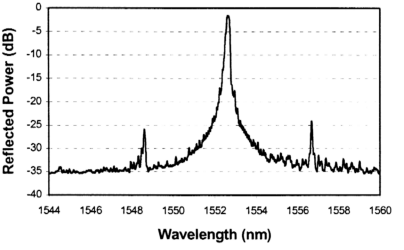

Figure 5.2: Reflection profile of FBG

the amplified spontaneous emission (ASE) is attenuated and controlled in the feedback loop by the attenuator.

The system is pumped through a WDM at 980nm by a laser diode. The pumping scheme is referred to as co-pumping since the signal and pump propagate in the same direction. The 13m length of EDF with a cut-off wavelength of 950nm, core refractive index of 1.473 and Er^{3+} concentration of +240ppm is used as a gain medium. The probe signal from an external cavity tunable semiconductor laser (TLS, Anritsu MG 9638A) and the reflected part of the ASE from the feedback loop are coupled into the system from the 90% port and 10% port of the coupler respectively. The output signal from the FBG is monitored with an optical spectrum analyzer (OSA, Anritsu MS 9710B).

For comparison, we also take the data of the same amplifier without laser oscillation (open system) by opening the feedback loop. In this open system, the circulator and FBG are removed.

5.2.2 Pump power

The effects of the 980nm pump power on the amplifier performance for FBG-clamped and open system are investigated in this experiment. The pump power P_P is increased up to a maximum of 108.8 mW. The signal wavelength λ_S is fixed at 1550nm with an input signal power P_{sig} of –30.0 dBm, which would operate the amplifier in the unsaturated regime. For the FBG-clamped system, the oscillating laser wavelength λ_L is the Bragg wavelength of the FBG that is 1552.6nm.

The output signal power P_{sout} as a function of pump power P_P is shown in Figure 5.3. In the FBG-clamped system, the output signal power increases with pump power at

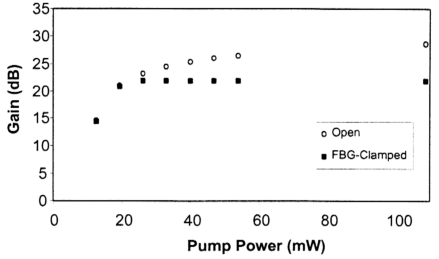

Figure 5.3: The output signal power P_{sout} as a function of pump power P_P. The points in between were omitted as they showed the same trend.

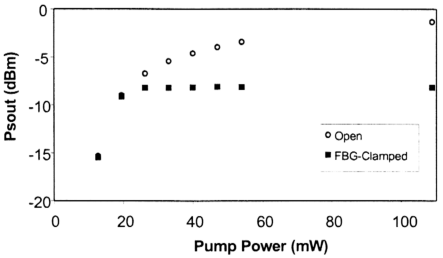

Figure 5.4: The signal gain as a function of pump power. The points in between were omitted as they showed the same trend.

low pump regions, and then saturated at P_{sout} = -8.2dBm when the pump power, P_p > 26.3mW. Above this pump power, there is no further amplification of the probe signal. The open system, without any oscillating laser, exhibits continuous increment of output signal power even at high pump powers. It gives a maximum output signal power of – 1.32dBm at the maximum pump power. Photons originating from the metastable state amplify the signal mode, besides being emitted as a spontaneous emission.

In Figure 5.4, the signal gain is plotted as a function of pump power. In the FBG-clamped system, the signal gain increases with pump power at low pump powers. This can be attributed to the increment of population inversion along the fiber with pump power. It is then clamped at a gain of 21.8dB when the P_p > 26.3mW due to the onset of laser oscillation at λ_L = 1552.6nm so that a constant average population inversion is maintained. The open system however exhibits continuous increment of gain. Signal gain as high as 28.7dB is achieved at the maximum pump power of 108.8mW. The open system does not exhibit the phenomena of gain clamping due to the continuous increment of the upper level, N_2, by the pump power as it increases. Therefore, the probe signals are amplified even at high pump powers. Theoretically, the gain of the open system would not increase infinitely with pump power due to amplifier self saturation, which eventually results in gain saturation [11]. This is not observed in this study because the available pump power is insufficient.

Figure 5.5 shows the noise figure as a function of pump power. The noise figure for the FBG-clamped system decreases slightly with pump power. The lowest noise figure that can be obtained by the system is 5.4dB at the maximum pump power of 108.8mW. The noise figure for the open system shows the opposite behavior. It increases

slightly with pump power. The lowest noise figure is 5.9dB at the minimum pump power of 12.8mW. It also can be observed that the FBG-clamped system exhibits noise figures much lower than the open system. It shows that the presence of the oscillating laser has an effect on noise figure, in which the ASE power is strongly suppressed by the laser power and the operation point of the amplifier fell in the dip region of the original noise profile, which has been detailed previously in [12].

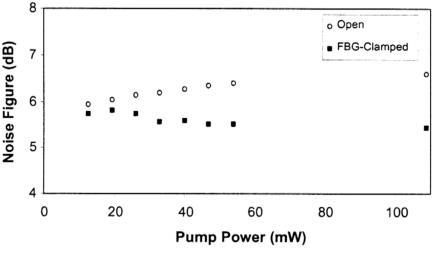

Figure 5.5: The noise figure as a function of pump power. The points in between were omitted as they showed the same trend.

5.2.3 Input signal power

The effect of increasing the input signal power on the amplifier performance parameters such as output signal power P_{sout}, signal gain G and noise figure NF is investigated for the FBG-clamped system and the open system. For the FBG-clamped system, the investigation is done for various attenuation of fedback laser power. The

input signal wavelength λ_{sin} and the pump power P_p are fixed at 1550nm and 108.8mW, respectively.

Figure 5.6 shows the powers of the amplifier spectrum for different input signal power with optical feedback power attenuation of 2dB. The power of the oscillating signal drops with increasing of P_{sin} until it saturates at a high input power. Figure 5.7 illustrates the output signal power as a function of input signal power. P_{sout} increases linearly at low input signal and exhibits the same power at high input power.

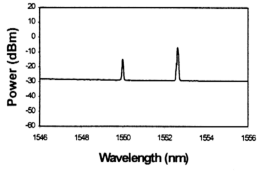

(a) P_{sin} = -40dBm

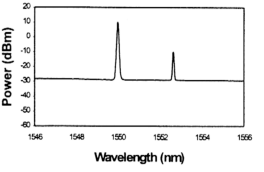

(b) P_{sin} = -15dBm

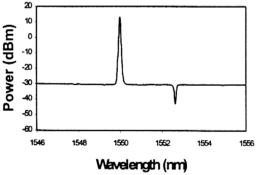

(c) P_{sin} = -10dBm

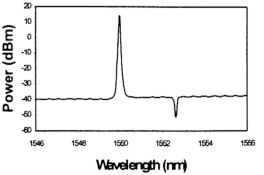

(d) P_{sin} = 5dBm

Figure 5.6: Powers of the amplifier spectrum for different input signal power

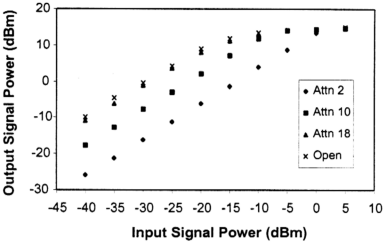

Figure 5.7: Output signal power as a function of input signal power

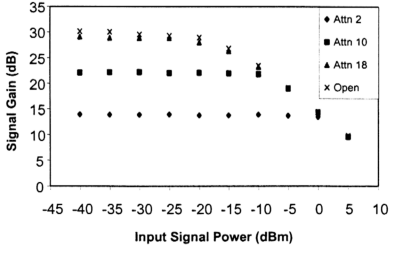

5.8: Signal gain as a function of input signal power

Figure 5.8 shows the effect of increasing the input signal power on the signal gain. In the small signal regime (i.e P_{sin} < -10dBm for attenuation = -10dB), the signal gains are flat. This flat regime is usually denoted as an unsaturated regime where the signal gain is independent of input signal power P_{sin}. At smaller attenuation, the feedback laser power is high, and it can give a broader unsaturated regime, but the gain maximum is smaller. As the power of feedback laser increases, the competition between the laser and signal mode increases which contributes to the degradation of the signal gain. Above this flat regime, the gain starts to decrease or saturate linearly. The effect of gain saturation occurs when the stimulated emission rate induced by the high input signal power becomes equal or takes over to the pumping rate. Therefore, the metastable level is emptied faster than that it is filled by the pump [13]. The gain maximum is 13.9dB, 22.2dB and 29.1dB, 30.1dB for the attenuation of 2dB, 10dB,18dB and an open system, respectively. The critical input power for attenuation of 2dB, 10dB,18dB and the open system are 0dBm, -10dBm, –20dBm and –20dBm, respectively. The critical input power is defined as the maximum input power below which the amplifier gain can be maintained at a constant level.

Figure 5.9 shows the noise figure as a function of input signal power.In the small signal regime where P_{sin} < -10dBm, the noise figure is does not change much. In this regime, the highest noise figure is 6.5dB which is obtained from attenuation of –18dB. The noise figure increased drastically at high input signal powers (P_{sin}>-5dBm) due to the depletion of upper level population by the strong input power, where the gain is also low.

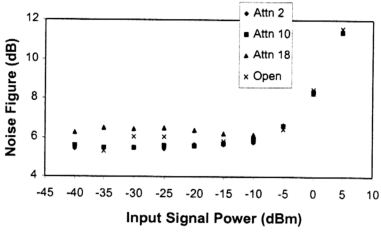

Figure 5.9: Noise figure as a function of input signal power

5.2.4 Effect of feedback laser power attenuation

The effect of feedback laser power attenuation on the amplifier gain and noise figure is investigated in this experiment. The laser power is attenuated from 2 to 18dB for various input signal power from -40 to 5dBm. The signal wavelength and pump power are fixed at 1550nm and 108.8mW, respectively.

The signal gain as a function of attenuation for various input power is shown in Figure 5.10. The signal gain increases linearly with attenuation at low attenuation regions and then saturates at high attenuation regions. For example, at P_{sin} = -10dBm, it increases with attenuation until the attenuation reaches 12dB and then saturated at gain of -23.2dBm. As the attenuation increases, the power of the oscillating laser reduces and it contributes to reduction in mode competition, which causes the gain to increase until the saturated region is reached. Figure 5.11 shows the noise figure as a function of attenuation for various input power. The noise figures are fluctuating in the unsaturated regions and are constant in the saturated regions. For example, at P_{sin} = -10dBm, the noise

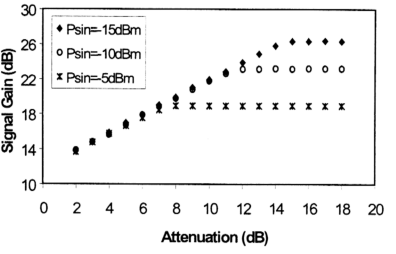

Figure 5.10: Signal gain as a function of attenuation for various input power

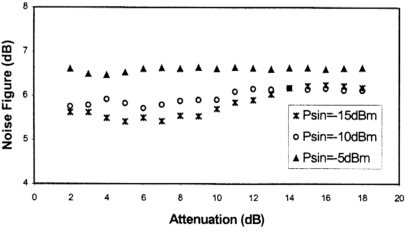

Figure 5.11: Noise Figure as a function of attenuation for various input power

figure fluctuates with attenuation until the attenuation of 14dB, and then stays constant below 6.2dB. After an attenuation of 14dB, the noise figure remains constant since there is no laser oscillation in the cavity. The noise figure fluctuating is caused by the FBG thermo-optic instability.

5.3 Fiber Bragg grating laser

5.3.1 Experimental set up

The experimental set up of the Bragg grating fiber laser is shown in Figure 5.12. The laser system consists of a section of an erbium-doped fiber (EDF), a 980/1550nm wavelength division multiplexer (WDM), a four port optical circulator, a fiber Bragg grating (FBG) and a 3dB coupler. The EDF of length 4.65m, cut-off wavelength of 950nm, refractive index of 1.473, core diameter of 1.68μm and ion concentration of +240ppm is used as an active gain medium in the fiber laser system. The FBG used in this experiment has been fabricated in high germania boron co-doped silicate fiber by a continuous wave argon ion laser at 244nm with a phase mask method as detailed in the previous chapter. A 980nm diode laser pump is coupled into the EDF by a WDM. An optical circulator is used to incorporate a fiber grating into the laser cavity as a narrow linewidth filter and to ensure unidirectional laser operation as well as to avoid driving relaxation oscillations in the cavity. The optical circulator is made by KAIFA Technology Inc and has a low insertion loss of ~1dB between any two ports. A 3dB wide band coupler (WBC) is used as an output coupler. The output power is measured by an optical spectrum analyzer (OSA, Anritsu MS9710B).

The FBG laser was characterized for different FBG reflectivities. The laser wavelength is also tuned using a heater to detune the Bragg resonance wavelength of the FBG. The pump power is varied from 0 to a maximum power of 46.2mW during the experiment.

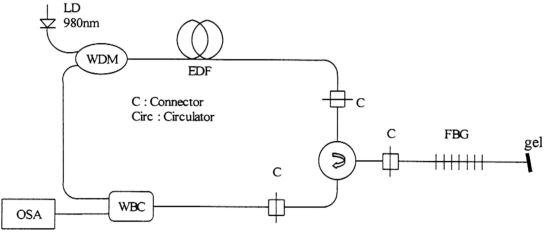

Figure 5.12: Experimental set up of fiber Bragg grating laser

5.3.2 FBG laser characterization

In this experiment, the FBG laser characteristics such as pump threshold, slope efficiency, total output power etc. are investigated for different FBG reflectivities. Four FBGs are used and investigated in this experiment. The parameters of these FBGs are shown in Table 5.1. The grating reflectivity were measured using a method that described in chapter IV. The reflection profile of the each FBGs are shown in Figure 5.13.

FBG	Reflectivity (%)	3dB bandwidth (nm)	Bragg Wavelength (nm)
1	35.7	0.13	1553.12
2	82.5	0.24	1553.22
3	97.4	0.32	1553.39
4	99.9	0.84	1553.75

Table 5.1: The fiber Bragg grating parameters

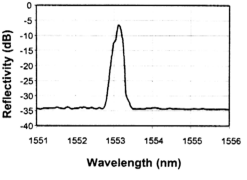

(a) FBG 1

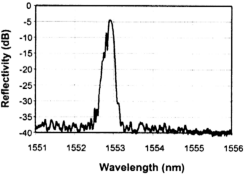

(b) FBG 2

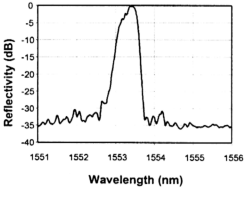

(c) FBG 3

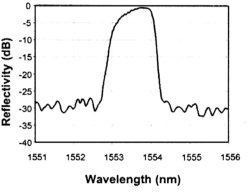

(d) FBG 4

Figure 5.13: Reflection profile for different fiber Bragg grating

Figure 5.14 shows the output power as a function of pump power for using FBG's 1 to 4. The output spectrum when pumped by a maximum pump power of 46.2mW is shown on Figure 5.15. A peak laser power for a maximum pump power, lasing wavelength, laser linewidth, pump threshold power and slope efficiency are determined from these figures and summarized in Table 5.2. It shows that the higher reflectivity FBG gives a higher peak power as well as slope efficiency except for FBG 4. Slope efficiency is the efficiency of laser to convert the pump power into laser power once it has reached threshold [8], [9], [10]. Increment of the grating reflectivity means increase in intensity of the circulating light in the cavity. Stimulated emission rate now increases due to more stimulated photons in oscillation. This then results in a higher output power as well as better slope efficiency.

The difference in result for FBG 4 is because it has the highest reflectivity of 99.9% and the broadest 3dB bandwidth of 0.84nm. There are two modes present in the cavity at high pump power as shown at Figure 5.15(d). When the pump power is increased there is a tendency for a second mode to oscillate. The laser power against pump power for these two modes is shown in Figure 5.16. The slope efficiencies for dominant mode and second mode are 8.95% and 1.59% respectively. This two mode spectral structure is suspected to be due to gain competition in the gain medium [14]. The stable simultaneous oscillating modes indicate weak coupling between them [8]. Once a mode exceeds threshold, the gain of the mode is clamped at the value of loss. Since the gain is wavelength dependent and not entirely homogeneous (spatially and spectrally), it is possible for other modes to reach threshold and begin oscillating at higher pump powers. Therefore, the dominant mode increases linearly with pump power until it has

been saturated once it reaches the saturated region. Once the dominant mode saturates, the second mode starts to grow.

FBG	Peak power (dBm)	Lasing Wavelength (nm)	Linewidth (nm)	Threshold (mW)	Slope Efficiency (%)
1	1.28	1553.072	0.01	5.02	3.25
2	5.16	1553.206	0.02	3.62	7.76
3	7.28	1553.348	0.02	3.43	12.51
4	6.06	1553.657	0.01	1.53	8.95

Table 5.2: The summary of fiber laser characteristics under different FBGs

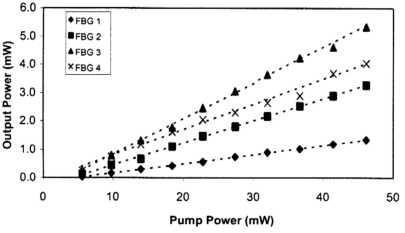

Figure 5.14: Laser output power as a function of pump power

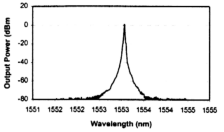

(a) FBG 1

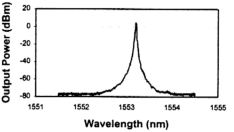

(b) FBG 2

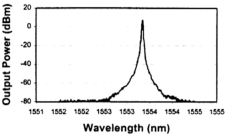

(c) FBG 3

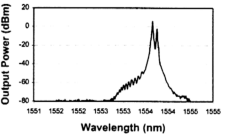

(d) FBG 4

Figure 5.15: Laser Output Spectrum for different FBG

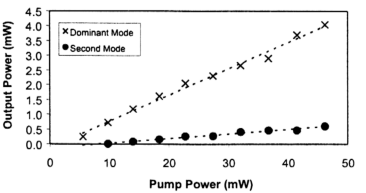

Figure 5.16: Laser power as a function of pump power for FBG 4

The pump power threshold shows an opposite behaviour where it decreases with the FBG reflectivity. Laser threshold is determined at the point where gain equals total cavity loss during a round trip [8], [9], [10]. Total cavity loss is smaller with the higher reflectivity FBG, therefore the threshold decreases with the reflectivity. The overall laser threshold is extremely low since it takes little pump power to almost fully invert the Er^{3+} ions. Lasing occurred at around 1553nm, corresponding to the Bragg resonance wavelength. However the lasing wavelength is slightly longer than the fiber grating center wavelength. The fiber lasers have a spectral width of 0.01 ~ 0.02nm limited by the resolution of the OSA and a lasing output peak to background noise of 46 ~ 78dB irrespective of the grating reflectivity.

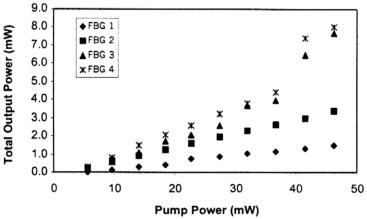

Figure 5.17: Total output power as a function of pump power

The total output power as a function of pump power for using FBG 1 ~ 4 is shown on Figure 5.17. The total output power increases linearly with pump power with the higher reflectivity FBG giving a better slope. Population inversion in the EDF

increases with grating reflectivity increment. Thus, any given pump power can be converted into a larger laser power.

The FBG laser output power as well as slope efficiency can be improved by increasing the EDF length, using higher erbium concentration EDF and reducing the cavity loss. The FBG laser operates as a three level laser system when excited by a 980 nm pump laser so that a length of unpumped fiber absorbs strongly at the lasing wavelength. For a given fiber length, lasing can occur only if the gain available from the bleached section equals, or exceeds, the loss of the remaining length. This means fiber length is a very important parameter in the design of the FBG laser. The use of high concentration EDF will increase the absorption per unit length and it can reduce the EDF length requirement of the laser. The low cavity loss increases the oscillating laser power in the cavity.

5.3.3 Fiber laser tuning

Many techniques have been used to tune the FBG laser. The commonly used techniques are either stretching or compression [15], [16]. Pan et al. shows that a tuning range of 18 nm was obtained by compressing FBG in specially designed unit with an optical circulator [16]. The ability to control relaxation oscillations associated with wavelength tuning, which limit the effectiveness of tuning in fiber lasers, has led to extensive development of FBG lasers [17].

Tuning of the fabricated FBG laser is demonstrated by temperature tuning of Bragg wavelength of grating. The FBG section of the laser system is put into an electric furnace. The furnace temperature is set to temperatures varying from 30 to 130°C.

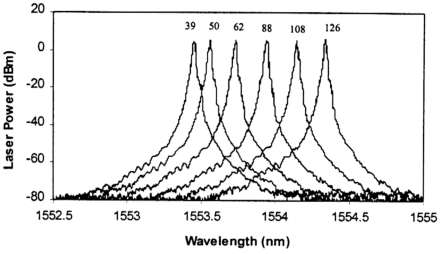

Figure 5.18: Spectra of the tuned erbium-doped fiber laser

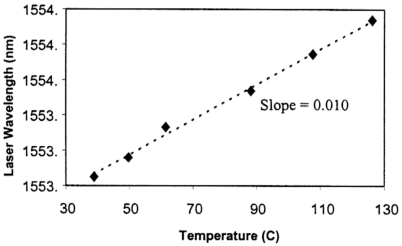

Figure 5.19: Variation of fiber laser wavelength with temperature

After it reaches the setting temperature, the reading is taken after waiting for 10 minutes in order to keep the FBG region at a constant temperature. The setting temperature is confirmed again with two independent thermometers to make sure that the applied temperature being distributed uniformly along the FBG. Figure 5.18 shows the output

tuning spectra for the fiber laser. Simultaneous temperature tuning demonstrates a 0.01nm/°C variation in laser wavelength as shown in Figure 5.19. A continuous tuning range of 0.9 nm is obtained by varying the fiber temperature from 39 to 126°C. It is expected that an improved tuning range and tuning response would be found using a grating stretcher or strainer.

References

1. C.R. Giles, J. Stone, L.W. Stulz, K. Walker, and C.A. Burrus, "Gain enhancement in reflected-pump erbium-doped fiber amplifiers," in Tech. Dig. Optic. Amplifiers and Their Applications, Vol.13, paper ThD2, pp.148-151,1991.

2. J.L. Zyskind, J.W. Sulhoff, P.D. Magill, K.C. Reichmann, V. Mizrahi, and D.J. DiGiovanni, "Transmission at 2.5Gbit/s over 654km using an erbium-doped fiber laser source," Electron. Lett., Vol.29, No.12, pp.1105, 1993.

3. A.J. Stentz, T. Nielsen, S.G. Grubb, T.A. Strasser, and J.R. Pedrazzani, "Raman ring amplifier at 1.3μm with analog-grade noise performance and an output power of 23dBm," in Proc. OFC'96, paper PD 16, pp.391-394, 1996.

4. C.R Giles, R.D. Feldman, T.H. Wood, M. Zirngibl, G. Raybon, T.Strasser, L. Stulz, A. McCormick, C.H. Joyner, and C.R. Doerr, "Access PON using downstream 1550-nm WDM routing and upstream 1300-nm SCMA combining through a fiber-grating router," IEEE Photon. Technol. Lett., Vol.8, pp.1549-1551, Nov 1996.

5. C.R. Giles and V. Mizrahi, "Low-loss add/drop multiplexer for WDM lightwave networks," in Proc. IOOC'95, paper ThC2-1, Hong Kong, 1995.

6. W.H. Loh, R.I. Laming, A.D. Ellis, and D. Atkinson, "Dispersion compensated 10 Gbit/s transmission over 700 km of standard single mode fiber with 10 cm chirped fiber grating and duobinary transmitter," in Proc. OAA'96, paper PD30-2, 1996.

7. J.L. Zyskind, Y. Sun, A.K. Srivastava, J.W. Sulhoff, A.J. Lucero, C. Wolf, and R.W. Tkach, "Fast power transients in optically amplified multi wavelength optical networks," Optical Fiber Communication, Tech. Dig., Opt. Soc. Amer., Vol.2, pp.451-454, paper PD31-1, 1996.

8. A.E. Siegman, "Lasers," University Science Books, Mill Valley, California, 1986.

9. P.W. Millonni and J.H. Eberly, "Lasers," Wiley, New York, 1988.

10. B.E.A. Saleh and M.C. Teich, Fundamentals of Photonics, Wiley, New York, 1991.

11. E. Desurvire, "Erbium-Doped Fiber Amplifiers: Principles and Applications," John Wiley and Sonc, Inc, 1994.

12. R.I Laming, J.E. Townsend, D.N. Payne, F. Meli, G. Grasso, E.J. Tarbox, "High Power Erbium-Doped Amplifiers Operating in the Saturated Regime," IEEE Photon. Tech. Lett., Vol.3, No.3, pp.253, 1991.

13. M.P. Petrov, R.V. Kiyan, E.A. Kuzin, E.A. Rogacheva and V.V. Spirin, "Gain Saturation in three- and four-level fiber amplifiers," Opt. Comm., pp.109, 1994.

14. R. J. Mears, " Fiber lasers and amplifiers," PhD thesis, University of Southamton.

15. G. A. Ball and W. W. Morey, "Continuously tunable single-mode erbium fiber laser," Opt. Lett., Vol. 17, pp. 420-422, 1992.

16. J. J. Pan and Yuan Shi, "Tunable erbium-doped fibre ring laser using fibre grating incorporated by optical circulator or fibre coupler," Electron. Lett. Vol. 31, No. 14, pp. 1164-1165, 1995.

17. Y. T. Chieng and G. J. Cowle, "Suppression of relaxation oscillations in tunable fiber lasers with a nonlinear amplified loop mirror," IEEE Photon. Tech. Lett., Vol. 7, No. 5, pp. 485-487, 1995.